— Regular Article —

A Single Instillation of Amorphous Silica Nanoparticles Induced Inflammatory Responses and Tissue Damage until Day 28 after Exposure

Eun-Jung Park,*[,a] Jinkyu Roh,[b] Younghun Kim,[b] and Kyunghee Choi[a]

[a]*Environmental Health Risk Research Department, National Institute of Environmental Research, Kyungseo-dong, Seo-gu, Incheon 404–708, Korea and* [b]*Department of Chemical Engineering, Kwangwoon University, 447–1, Wolgye-dong, Nowon-gu, Seoul 139–701, Korea*

(Received September 29, 2010; Accepted November 2, 2010)

Synthetic amorphous silica nanoparticles (SiNPs) are seeing increased and widespread application in diagnosis, imaging, and drug delivery. In the present study, the inflammatory responses and histopathological changes caused by inflowing of SiNPs into the lung were studied in mice after a single intratracheal instillation. Changes in gene expression were also investigated in lung tissue using microarray analysis. As results, weight gain was significantly decreased in SiNP-treated mice on day 1 and 7 after instillation. The secretion of pro-inflammatory cytokines [interleukin (IL)-1, IL-6, and tumor necrosis factor (TNF)-α] and transforming growth factor (TGF)-β were also increased, and the distribution of cytotoxic T cells, natural killer (NK) cells, and natural killer T (NKT) cells with G1 arrest were increased. Microgranulomatous changes were observed on day 7 and 14. Furthermore, the gene expression was significantly affected on day 7. A total of 331 genes were up-regulated more than 2 fold, and 128 genes were down-regulated more than 2 fold. The secretion of inflammatory related cytokines, histopathological abnormalities, and the severity of gene expression changes decreased in a time-dependent manner. Based on these results, we suggest that SiNPs induce subchronic inflammatory responses and tissue damage in mice after a single intratracheal instillation.

Key words —— amorphous silica nanoparticle, inflammation, cytokine, gene expression

INTRODUCTION

Silicas (SiO_2) are the most abundant components of the earth's crust except carbon, and they can be divided into crystalline or non-crystalline (amorphous) forms. Crystalline silica is known to cause adverse health effects such as silicosis,[1–3] whereas amorphous silicas, being generally free of crystalline forms, are considered to be less toxic. Consequently, amorphous silicas, in the form of synthetic amorphous silica nanoparticles (SiNPs), are used in the production of various consumer goods, such as whiteware, cement, food additives, electric insulators, toothpaste, and tires. Recently, the application of nanoparticles has rapidly increased to diagnosis, imaging, and drug delivery, SiNPs are also widely using in diagnostic and biomedical research because of their ease of production and relatively low cost.[4,5]

On the other hand, many toxicologists have reported that SiNPs can cause adverse health effects depending on their manufacturing process. In a previous study, SiNPs inhibited the growth of the green alga, *Pseudokirchneriella subcapitata*.[6] SiNPs also induced cytotoxicity via oxidative stress in different types of cultured cell lines.[7–10] Moderate to severe pulmonary inflammation was observed in mice intratracheally instilled with ultrafine silica particles,[11,12] and the viability of splenocytes harvested from the mice treated with SiNPs was also significantly decreased in a high-dose treated group.[13] In addition, instillation of SiNPs stimulated cytokine secretion, induced the expression of matrix metalloproteinases (MMPs) and a tissue inhibitor of metalloproteinases (TIMP-1), and caused transient

*To whom correspondence should be addressed: Environmental Health Risk Research Department, National Institute of Environmental Research, Kyungseo-dong, Seo-gu, Incheon 404–708, Korea. Tel.: +82-32-560-7174, Fax: +82-32-568-2037; E-mail: pej303@korea.kr

fibrosis.[14)]

Furthermore, nanoparticles stimulate various immune cells in there when entered into the body, and disturb normal immune balance. Nanoparticles remained in lung tissue also may continuously impair lung tissue, and cellular interactions with nanoparticles are dependent on their unique physico-chemical properties including size, shape, surface characteristics, degradation, agglomeration, and surface charge. However, studies on the interactions between nanoparticles and cell biology based on the information on their unique physicochemical properties are in infancy.[5, 15, 16)]

In the present study, we identified the physicochemical properties of SiNPs and then explored both inflammatory responses and histopathological changes until day 28 after a single instillation into mouse's lungs to evaluate their potential toxicity. We also investigated global changes in gene expression following SiNP instillation using microarray analysis.

MATERIALS AND METHODS

Preparation of Test Material —— SiNPs (Aerosil®200, Degussa, Parsippany, NJ, U.S.A.) were dispersed using a sonifier (ULH-700S, Sibata, Soka, Japan), and particle size of the dispersed preparation was measured by a submicron particle sizer (NICOMPTM, Santa Barbara, CA, U.S.A.). Images were acquired by transmission electron microscopy (TEM; JEM1010, JEOL, Tokyo, Japan), and the surface charge was measured using a zeta potential analyzer (Brookhaven Instruments Corp., Holtsville, NY, U.S.A.).

Animals —— ICR mice 5 weeks of age (body weight 25 ± 1 g) were purchased from Orient-Bio Animal Company (Seongnam, Gyunggi-do, Korea) and were adapted to the animal room conditions for one week prior to initiation of the study. The environmental conditions were a temperature of 23 ± 1°C, relative humidity of 55 ± 5%, and a 12/12 hr light/dark cycle. All animals used in this study were cared for in accordance with the principles outlined in the "Guide for the Care and Use of Laboratory Animals" issued by the Animal Care and Use Committee of the National Veterinary Research and Quarantine Service (NVRQS). Body weights were measured on the treatment day and on scheduled time points using control group mice and the day 28 treatment group.

Intratracheal Instillation and Sample Preparation —— To investigate time-dependent changes induced by intratracheal instillation, SiNPs (1 mg/kg, 90–100 μl/mouse) were delivered with a 24-gauge catheter by intratracheal instillation under light tiletamine anesthesia (zoletil 50, Virbac Lab, Carros, France, Day 0). The control group was instilled with phosphate buffered saline (PBS, n = 12). Mice were sacrificed on day 1, 7, 14, and 28 after treatment (n = 12 per each time point). Sacrifice for biological sampling of day 1 was performed on 24 hr after instillation. At the selected time intervals after instillation, about 1 ml of blood per mouse was collected from the retro-orbital venous plexus into heparinized capillary tubes.

Whole blood (100 μl) was separated for cell phenotype analysis of blood lymphocytes, and the rest of the blood was centrifuged at 3000 rpm for 10 min. Serum from 4 mice (300 μl per mouse) was pooled to make one test sample. Three test samples were prepared for cell phenotype, cytokines, and IgE assay.

Bronchoalveolar lavage (BAL) fluid was obtained by cannulating the trachea and lavaging the lungs with 1 ml of cold sterile (Ca^{2+} plus Mg^{2+})-free PBS (0.15 M, pH 7.2). Approximately 500–600 μl BAL fluid was harvested per mouse, and BAL fluid from 4 mice (400 μl per mouse) was pooled to make one test sample. This was separated into BAL cells and supernatant by centrifugation at 3000 rpm for 10 min. Three test samples were prepared for cell cycle, cytokines, and IgE assay.

Cell Cycle Analysis —— BAL cells were stained using propidium iodide and ribonuclease (RNase) purchased from Sigma-Aldrich (St. Louis, MO, U.S.A.). The cell cycle was analyzed by measuring DNA content with the FACSCalibur system and CellQuest software (BD Biosciences, Franklin Lakes, NJ, U.S.A.). Cell cycle analysis was performed three times and representative data are presented.

Measurement of Cytokines and IgE —— The concentration of each cytokine in the supernatant of the BAL fluid and serum was determined using commercially available ELISA kits (eBioscience, San Diego, CA, U.S.A.). Briefly, each well of a 96 well plate was coated with 100 μl of capture antibody, and incubated overnight at 4°C. After washing and blocking with assay diluents, a volume of BAL fluid, serum, or standard was added to individual wells, and the plates were maintained for 2 hr at room temperature. Biotin-conjugated detecting

mouse antibody was then added to each well and incubated at room temperature for 1 hr. The plates were then incubated with avidin-HRP for 30 min before detection with TMB solution. Reactions were stopped by adding 1 M H_3PO_4, and the absorbance at 450 nm was measured with an ELISA reader (Molecular Devices, Sunnyvale, CA, U.S.A.). The amount of cytokine was calculated from the linear portion of a generated standard curve.[13)]

The concentrations of IgE in serum and BAL fluid were determined using commercially available IgE ELISA kits (Komabiotech, Seoul, Korea). Briefly, each microplate well was coated with coating antibody and incubated overnight at 4°C. The wells were blocked with blocking solution for 1 hr at room temperature. BAL fluid, serum, or a standard were added to individual wells and left for 1 hr at room temperature. The detection antibody was added to each well and the plates were incubated at room temperature for 1 hr. After washing, the plates were further incubated with a color development solution for 15 min. Finally, the reaction was terminated by the addition of 2 M H_2SO_4, and the absorbance was measured at 450 nm with an ELISA reader (Molecular Devices). The amounts of secreted IgE were calculated from the linear portion of the prepared standard curve.

Immunophenotyping —— All monoclonal antibodies were purchased from eBioscience. T cells (CD3, 1 : 50), B cells (CD19, 1 : 50), natural killer (NK) cells (DX5, 1 : 100), CD4+ T cells (CD4+, 1 : 160), and CD8+ T cells (CD8+, 1 : 50) were identified using directly conjugated anti-mouse antibodies. The blood was lysed for 5 min with fluorescence-activated cell sorting (FACS) lysis buffer (BD Bioscience) at room temperature and then re-washed with FACS buffer. Finally, each sample was fixed with 1% paraformaldehyde until further analysis. Flow cytometry analysis was performed on the FACSCalibur system (BD Biosciences). Control samples were matched for each fluorochrome. Data were analyzed using CellQuest software (Becton Dickinson, Franklin Lakes, NJ, U.S.A.).[17)] The experiment was performed three times and representative data were presented.

Histopathology —— Histopathological analysis was the responsibility of a pathologist in Biotoxtech (Cheongwon-gun, Chungbuk, Korea), one of the good laboratory practice (GLP) institutes in Korea. Briefly, lungs from mice of the control and the treated group were fixed with 10% neutral buffered formalin and processed using routine histological techniques. After paraffin embedding, 3 μm sections were cut and stained with hematoxylin and eosin (H&E) for histopathological evaluation.

Table 1. Primer Sequences Used in this Study

Primer	GB NO.	Sequence
SAA3	NM 011315.3	(L): tgtggcgagcctactctgac
		(R): ctggcatcgctgatgacttt
MMP 11	NM 008606	(L): cccatgccttcttccctaag
		(R): gctgtggtgtgttgtagccc
MMP 19	NM 021412	(L): ggccagaactgaccttagcc
		(R): gagtaacgtccccggttgat
Timp 1	NM 011593	(L): tatgcccacaagtcccagaa
		(R): cctgatccgtccacaaacag
HSP 8	NM 031165	(L): tcacagtgcccgcttacttc
		(R): gcagcagcagttggttcatt

Gene Expression of Tissue —— Using the RNAgent Total RNA Isolation System (Promega, Madison, WI, U.S.A.), total RNA was prepared from the lung tissue of mice sacrificed at days 7 and 28 after instillation of SiNPs (1 mg/kg). Six lung tissues were pooled to make two samples from 12 mice. Microarray data for changes in whole gene expression was performed by Macrogen (Seoul, Korea) using Applied Biosystems Mouse Genome Survey Arrays. Briefly, digoxigenin-11-UTP labeled cRNA was generated. It was linearly amplified from 1 μg of the total RNA purified from the control and the SiNP group, using an Applied Biosystems Chemiluminescent RT-IVT Labeling Kit. Array hybridization, chemiluminescence detection, image acquisition, and analysis were performed using the Applied Biosystems Chemiluminescence Detection Kit and Applied Biosystems 1700 Chemiluminescent Microarray Analyzer, following the manufacturer's protocols. Each image was collected for each microarray using the 1700 analyzer, which was equipped with a high-resolution, large-format CCD camera for gene expression analysis. Images were auto-gridded and the chemiluminescent signals were quantified, corrected for background and spot, and spatially normalized.

RT-PCR to analyze individual gene expression was performed using total RNA prepared from the lung tissue of control and SiNP groups. Amplified cDNA products were separated on a 1.5% agarose gel by electrophoresis. Table 1 shows the primer list used in this experiment (Bioneer Co., Daejeon, Korea).

Statistical Analysis —— The results obtained from the chemically treated groups were compared to those of the control group. The values were com-

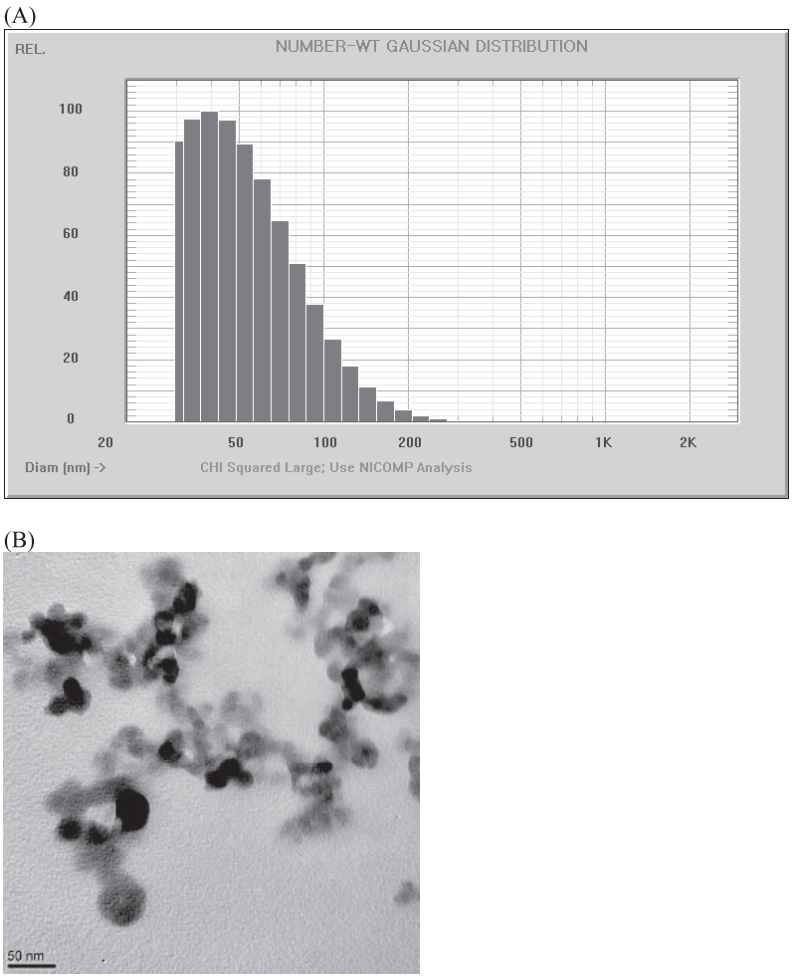

Fig. 1. Particle Size Distribution and TEM Images of SiNPs

Particle size was measured using a submicron particle size analyzer. The particle size in PBS was 47.6 ± 29.7 nm (mean ± S.D.), and the preparation seemed to be slightly aggregated. Y axis represents the relative distribution ratio of particle size (A). TEM image of SiNPs (B).

pared using a one-way ANOVA test and Student's *t*-test. Levels of significance were represented for each result. A p value of 0.05 was considered statistically significant.

RESULTS

Physico-chemical Properties of SiNPs

Particle size of SiNPs in the PBS preparation used for the instillation was 47.6 ± 29.7 nm (Fig. 1A), surface charge was −12.76 mV, conductance was 22737 μS, and average mobility was −1.00 (μ/s)/(V/cm). TEM micrographs confirmed that the SiNPs were mildly agglomerated in the PBS preparation (Fig. 1B).

Changes in Body Weight by a Single Instillation of SiNPs

As shown in Fig. 2, the average body weight

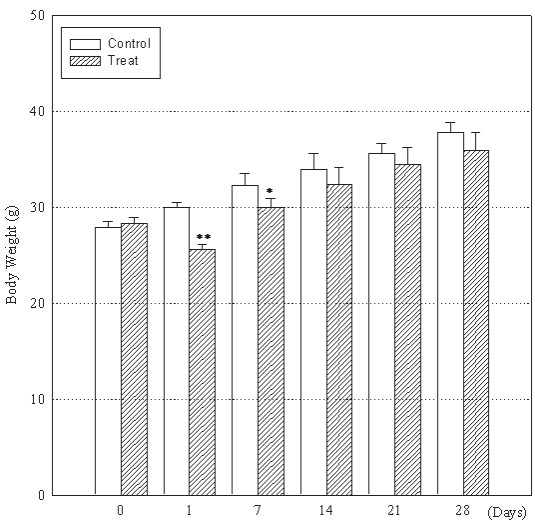

Fig. 2. Body Weight Changes in Mice Following Lung Instillation of SiNPs (n = 12)

Body weights were measured on days 0, 1, 7, 14, 21, and 28 after a single instillation of SiNPs (1 mg/kg). Day 0 designates the day of instillation. Significantly different from control group, $^{*}p < 0.05$, $^{**}p < 0.01$.

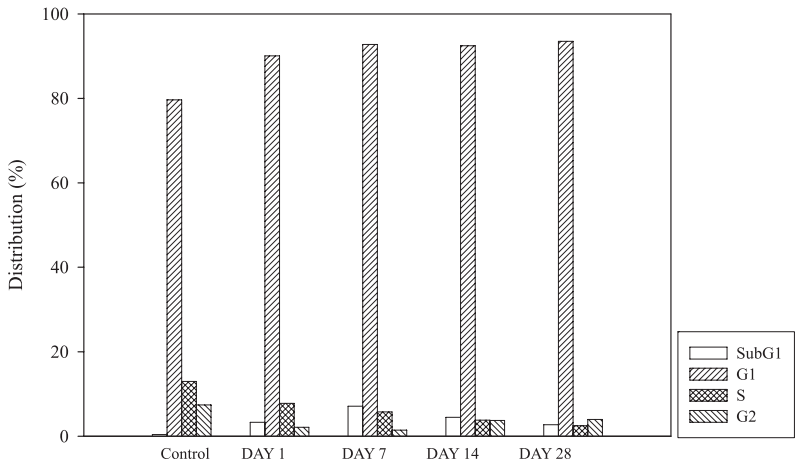

Fig. 3. Analysis of Cell Cycle Changes Following a Single Intratracheal Instillation of SiNPs

Mouse BAL cells were harvested at the designated times (days 1, 7, 14, and 28) following a single dose instillation of 1.0 mg/kg SiNPs (3 test samples were pooled from 4 mice, respectively, $n = 3$).

Table 2. Time-dependent Changes in Cytokine Levels in BAL Fluid Following Instillation of SiNPs

Significantly different from control group $^{*}p < 0.05$, $^{**}p < 0.01$.

	Control	Day 1	Day 7	Day 14	Day 28
IL-1β	0.30 ± 0.01	165.98 ± 8.96**	57.64 ± 2.36**	82.66 ± 0.99**	105.16 ± 6.31**
IL-6	0.90 ± 0.04	769.05 ± 73.83**	44.62 ± 0.58**	47.58 ± 2.00**	55.04 ± 2.37**
TNF-α	0.67 ± 0.06	156.66 ± 11.44**	33.53 ± 1.07**	13.77 ± 0.87**	19.90 ± 1.05**
IL-2	−0.15 ± 0.01	65.96 ± 4.22**	43.15 ± 3.54**	74.32 ± 10.26**	67.63 ± 1.89**
IL-12	−0.70 ± 0.02	193.48 ± 7.35**	285.01 ± 2.28**	96.43 ± 2.51**	107.87 ± 3.34**
IFN-γ	0.13 ± 0.01	26.11 ± 1.78**	20.17 ± 1.01**	13.53 ± 0.92**	17.10 ± 2.56**
IL-4	3.26 ± 0.33	81.89 ± 11.46	65.68 ± 8.01	67.71 ± 6.57	152.99 ± 12.70
IL-5	0.89 ± 0.11	46.01 ± 4.28	24.68 ± 2.15	28.06 ± 2.08	41.46 ± 2.24
IgE	2.18 ± 0.10	3.64 ± 0.22	5.51 ± 0.59*	2.54 ± 0.07	2.81 ± 0.08
TGF-β	5.14 ± 0.40	210.02 ± 28.14**	156.88 ± 3.92**	188.77 ± 10.00**	193.83 ± 23.84**

(± standard deviation) of the control group was 27.90 ± 0.58 g, while that of the SiNP group was 28.32 ± 0.58 g on day 0 (before treatment). However, body weight decreased rapidly after instillation on day 1, the average body weight of the SiNP group was 25.56 ± 0.58 g, while that of the control group was 29.96 ± 0.59 g. A gap between the control group and SiNP group was still observed until day 7, but the body weight of the SiNP group had recovered to the control weight by day 14.

Cell Cycle of the BAL Cell by a Single Instillation of SiNPs

Distribution of cells at the G1 stage in the control group was 79.64% and this increased to 96.03, 91.79, 92.82, and 93.89% on day 1, 7, 14, and 28 after instillation, respectively. The distribution of sub G1, which is related to cell apoptosis, increased significantly to 3.28, 7.1, 4.46, and 2.73% on day 1, 7, 14, and 28 after instillation, respectively, while that of control group was 0.41% (Fig. 3).

The Secretion of Cytokines and IgE by a Single Instillation of SiNPs

To observe time-dependent changes of cytokines related to the inflammatory responses and tissue damage, levels of pro-inflammatory cytokine [interleukin (IL)-1, tumor necrosis factor (TNF)-α, and IL-6], Th0-type cytokine (IL-2), Th1-type cytokine (IL-12 and IFN-γ), transforming growth factor (TGF)-β, and IgE were measured in BAL fluid (Table 2) and in serum (Table 3).

In the BAL fluid, the maximum level of pro-inflammatory cytokines (IL-1, TNF-α, and IL-6) was reached on day 1, and this level remained elevated during the entire experimental period. The secretion of IL-2 was rapidly elevated on day 1 and maintained a steady level during the experimental

Table 3. Time-dependent Changes in Cytokine Levels in Blood Following Instillation of SiNPs
Significantly different from control group $^{*}p < 0.05$, $^{**}p < 0.01$.

	Control	Day 1	Day 7	Day 14	Day 28
IL-1β	0.75 ± 0.02	3.17 ± 0.40	1.81 ± 0.10	2.72 ± 0.22	1.66 ± 0.14
IL-6	7.99 ± 0.77	114.03 ± 8.44**	8.51 ± 0.39	18.15 ± 0.80*	6.20 ± 0.45
TNF-α	0.51 ± 0.06	3.64 ± 0.18*	0.78 ± 0.12	0.57 ± 0.05	1.32 ± 0.08
IL-2	−1.07 ± 0.13	7.83 ± 0.98**	7.12 ± 1.05**	9.34 ± 0.93**	6.72 ± 0.42**
IL-12	42.25 ± 3.59	147.38 ± 5.01**	68.07 ± 0.88**	52.44 ± 3.78	87.74 ± 8.33**
IFN-γ	−1.25 ± 0.35	20.35 ± 3.26**	0.31 ± 0.07	−1.82 ± 0.27	−1.13 ± 0.08
IL-4	ND	ND	ND	ND	ND
IL-5	ND	1.68 ± 0.10	4.72 ± 0.01	5.25 ± 0.48	1.16 ± 0.18
IgE	6.60 ± 0.47	18.20 ± 1.13**	19.60 ± 0.56**	23.50 ± 0.15**	16.20 ± 0.98**
TGF-β	18.84 ± 2.13	24.40 ± 2.61	42.58 ± 3.62**	37.89 ± 1.06*	30.82 ± 4.16*

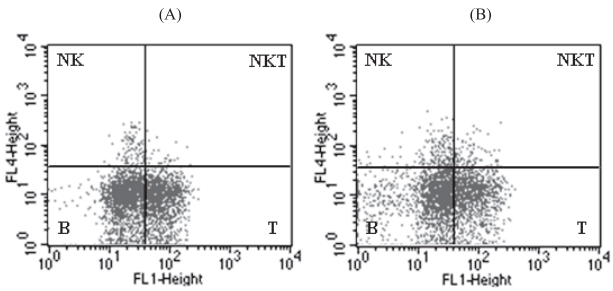

Fig. 4. Analysis of Lymphocyte Phenotypes Following a Single Instillation of SiNPs

Blood was harvested and pooled (3 test samples were pooled from 4 mice, respectively, $n = 3$) at day 1 following a single dose instillation of 1 mg/kg SiNPs. Flow cytometry analysis was performed a total of 3 times using the FACSCalibur system, and representative data are shown. Control samples were matched for each fluorochrome. (A): Control lymphocyte, (B): lymphocyte on day 1 following instillation.

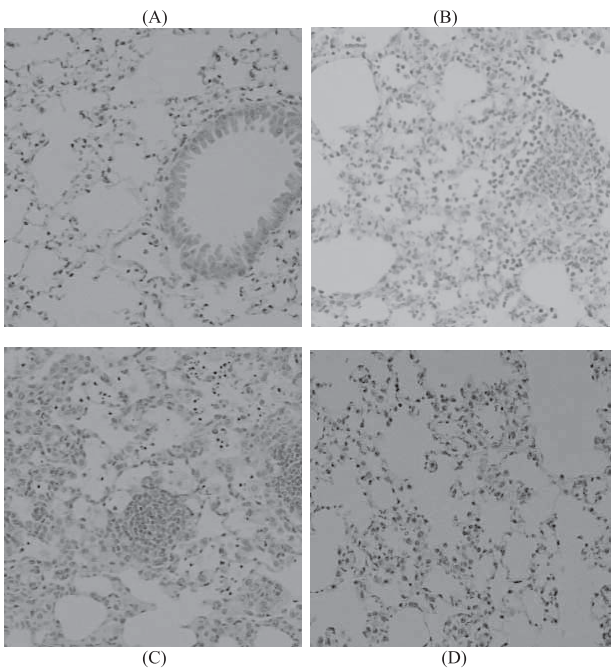

Fig. 5. Histopathology of Lung Tissues Following a Single Instillation of SiNPs

The lung tissue was harvested on days 1, 14, and 28 after a single dose instillation with 1 mg/kg SiNPs ($n = 3$). Three tissues per group were randomly selected and examined (× 200). (A); Control, (B); Day 1, (C); Day 14, (D); Day 28.

period. The levels of IL-12 reached their maxima on day 7. The maximum levels of TGF-β were reached on day 1 and the levels remained steady during the rest of the experimental period. An increase in IgE level was observed only on day 7 (Table 2).

In the serum, IL-6 and Th1-type cytokines (IL-12 and IFN-γ) showed peak levels on day 1, but the level decreased rapidly as time progressed. A mild increase in IL-2 was maintained throughout the experimental period. The secretion of TGF-β reached its maximum level on day 7, but no physiologically meaningful increases in IL-1 was seen in response to instillation of SiNPs (Table 3).

The Changes in Lymphocyte Phenotype by a Single Instillation of SiNPs

As shown in Fig. 4, the distributions of NK, NKT, B, and T cells on day 1 were 6.17, 3.31, 57.03, and 33.50%, respectively, in the SiNP group, and 3.46, 1.04, 53.45, and 42.06%, respectively, in the control group. The elevated levels of NK cell distribution was diminished in a time-dependent manner to 4.00, 2.98, and 2.74% on day 7, 14, and 28, respectively. The ratio of CD4+/CD8+ in the SiNP groups was 3.88, 3.14, 3.09, and 3.07 on day 1, 7, 14, and 28, respectively, and 3.81 in the control group, indicating that the distribution of cytotoxic T cells (CD8+) was increased.

Histopathology of Lung Tissue by a Single Instillation of SiNPs

Cell infiltration in the alveolar space and alve-

Table 4. Time-dependent Histopathological Changes Following a Single Instillation of SiNPs

Findings		Control	Day 1	Day 7	Day 14	Day 28
Microgranulomatous change, around	+	0	0	1	0	0
terminal bronchioles	++	0	0	2	1	0
Cell infiltration, alveolar macrophage	±	0	1	0	1	2
alveolar space	+	0	1	2	1	0
Cell infiltration, neutrophils, alveolar	+	0	1	1	0	0
space, alveolar wall	++	0	2	0	0	0
Cell infiltration, alveolar macrophage, Lymphocyte, mononuclear, neutrophils, alveolar space	+	0	0	1	0	0
Cell infiltration, mononuclear, around terminal bronchioles	±	0	0	0	1	0
Cell infiltration, mononuclear,	±	0	0	0	0	1
alveolar wall	++	0	0	0	1	0
Cell infiltration, mononuclear, alveolar wall, alveolar space	+	0	0	0	0	1
Cell debris, alveolar space	±	0	0	0	1	0

* Grade—±: minimal, +: mild, ++: moderate.

olar wall was observed throughout the experimental period, but the intensity decreased in a time-dependent manner (Fig. 5, Table 4). Moderate microgranulomatous changes around terminal bronchioles were observed on day 7 and 14. Histopathological changes were recovered to normal at three months after instillation (data not shown).

Gene Expression Changes Following a Single Instillation of SiNPs

Gene expression in lung tissue was investigated by microarray after a single instillation of SiNPs (1 mg/kg, Tables 5 and 6). A total of 331 genes including immunity- and defense-related genes (SAA3, E430002D04Rik, Ifi27, Orm1, and Oas1 g), chemotaxis-related genes (CCl4, Cxcl9, Il1rn, CCl3, Cxcl10, and CCl19), and major histocompatibility complex (MHC) class I-mediated immunity-related genes (H2-M2 and H2-Ab1) were up-regulated more than 2 fold on day 7. Genes involved in chromatin packaging and remodeling, such as Hist1h2ad, Hist1h2ah, Hist1h2af, Hist1h2ao, and Hist1h2an, were also up-regulated by SiNP instillation. A total of 128 genes were down-regulated more than 2 fold on day 7, including cytokine-related genes (Myh8 and Acta1), muscle contraction-related genes (Tnnc2, Myl1, Tpm2, Myl3, Mylpf, and Ckm), and MHC class II-mediated immunity-related genes (H2-Ea and H2-Eb1).

Based on microarray analysis, some genes which related to acute inflammatory responses and tissue damage were selected for RT-PCR analysis.

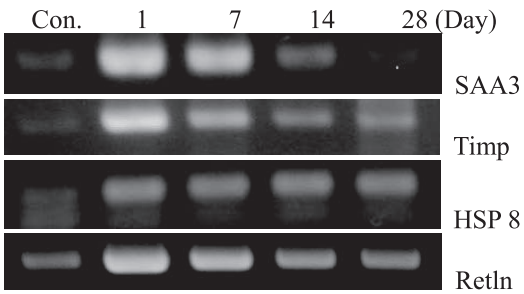

Fig. 6. Changes in Gene Expression Following a Single Instillation of SiNPs

RNA was extracted from the lungs of mice that had been treated with 1 mg/kg SiNPs at the designated time, and amplified by RT-PCR using primers described in Table 1. Results were confirmed by several separate experiments, and representative images are shown.

As shown in Fig. 6, the expression of serum amyloid A (SAA) 3, MMP-3, MMP-11, and TIMP were induced on day 1 after instillation. The elevated expression of these genes diminished as time progressed. However, the expression of heat shock protein (HSP) 8 was elevated on day 1 and remained elevated level throughout the rest of the experimental period.

DISCUSSION

Recently, application of SiNPs is more expanding from industrials to medical area including drug delivery, cancer theraphy, and pharmacy. It has been known since ancient times that inhaled crystalline silica particles cause silicosis, severe lung pneumo-

Table 5. Partial List of Up-regulated Genes in Lung Following a Single Instillation of SiNPs
This table contains genes up-regulated more 4 times than control group on Day 7.

Symbol	Day 7	Day 28	Biological Process
Saa3	60.11	15.33	Immunity and defense
Ccl4	12.10	2.96	Signal transduction
E430002D04Rik	11.84	4.68	Immunity and defense
Gpnmb	11.60	2.63	Biological process unclassified
Cxcl9	11.20	2.24	Signal transduction
AA467197	10.75	1.32	Other metabolism
Oas1g	10.04	2.38	Nucleoside, nucleotide and nucleic acid metabolism; Immunity and defense
Lcn2	9.74	3.97	Transport; Immunity and defense; Oncogenesis
H2-M2	9.46	2.14	Immunity and defense
Ifi27	8.92	3.35	Immunity and defense
Hist1h2ad	7.84	1.56	Nucleoside, nucleotide and nucleic acid metabolism
Hist1h2ah	7.56	1.37	Nucleoside, nucleotide and nucleic acid metabolism
Hist1h2ak	7.45	1.51	Nucleoside, nucleotide and nucleic acid metabolism
Cd177	6.75	5.64	Biological process unclassified
Prcp	6.60	5.55	Protein metabolism and modification
Prc1	5.93	1.42	Cell cycle
Timp1	5.72	1.52	Protein metabolism and modification; Developmental processes
Orm1	5.66	1.25	Immunity and defense
Ms4a7	5.66	3.40	Biological process unclassified
Ctsk	5.63	2.20	Protein metabolism and modification; Homeostasis
Hist1h2af	5.60	1.01	Nucleoside, nucleotide and nucleic acid metabolism
F10	5.52	1.45	Protein metabolism and modification
Oas1g	5.51	2.26	Nucleoside, nucleotide and nucleic acid metabolism; Immunity and defense
Hist1h2ao	5.40	1.04	Nucleoside, nucleotide and nucleic acid metabolism
Aif1	5.36	2.31	Immunity and defense; Cell cycle; Cell proliferation and differentiation
Il1rn	5.34	1.51	Signal transduction
Trem2	5.33	2.28	Biological process unclassified
Hist1h2an	5.31	1.04	Nucleoside, nucleotide and nucleic acid metabolism
Spp1	5.25	1.36	Cell adhesion; Cell structure and motility
Clec4n	5.23	2.07	Signal transduction; Cell adhesion; Intracellular protein traffic; Immunity and defense
Timp1	5.12	1.41	Protein metabolism and modification; Developmental processes
Retnla	5.08	−1.06	Biological process unclassified
Fcgr2b	5.06	1.56	Signal transduction; Immunity and defense
H2-Ab1	5.02	2.77	Immunity and defense
Slc26a4	5.01	3.45	Sulfur metabolism; Transport
Hk3	4.92	1.38	Carbohydrate metabolism
Ms4a6d	4.90	1.43	Biological process unclassified
Ccl3	4.88	2.03	Signal transduction; Immunity and defense
OTTMUSG 00000000971	4.87	1.14	
Il4i1	4.77	2.31	Electron transport
Gp2	4.69	−1.06	Intracellular protein traffic
Pbk	4.42	1.17	Protein metabolism and modification; Phosphate metabolism; Other metabolism
Irf7	4.42	1.41	Nucleoside, nucleotide and nucleic acid metabolism; Immunity and defense; Oncogenesis
Cxcl10	4.38	1.40	Signal transduction; Immunity and defense
Kng1	4.26	5.50	Immunity and defense; Blood circulation and gas exchange
Tnc	4.22	1.72	Signal transduction; Developmental processes
Tnc	4.20	1.88	Signal transduction; Developmental processes
Cd68	4.18	1.74	Biological process unclassified
Ccl9	4.17	1.83	Signal transduction
C1qc	4.11	2.48	Immunity and defense
Hist1h2ag	4.09	1.06	Nucleoside, nucleotide and nucleic acid metabolism
Clec4d	4.06	−1.34	Signal transduction; Cell adhesion; Intracellular protein traffic; Immunity and defense
Mmp12	4.02	2.64	Protein metabolism and modification
Arg1	4.01	1.31	Amino acid metabolism

Table 6. Partial List of Down-regulated Genes in Lung Following a Single Instillation of SiNPs
This table contains genes down-regulated more 3 times than control group on Day 7.

Symbol	Day 7	Day 28	Biological Process
Acta1	−28.81	−25.49	Intracellular protein traffic; Intracellular protein traffic; Transport; Cell cycle; Cell structure and motility
Myh8	−15.22	−15.94	Muscle contraction; Developmental processes; Cell cycle
Tnnc2	−9.59	−9.93	Signal transduction; Muscle contraction; Developmental processes
Lor	−8.62	−7.74	Biological process unclassified
Myl1	−7.99	−5.67	Muscle contraction
H2-Ea	−7.08	−17.77	Immunity and defense
Angptl7	−6.96	−15.97	Miscellaneous
Cyp2a5	−6.34	−6.24	Lipid, fatty acid and steroid metabolism; Lipid, fatty acid and steroid metabolism; Electron transport
Krt13	−6.23	−5.81	Cell structure and motility
Cyp2a5	−6.10	−7.64	Lipid, fatty acid and steroid metabolism; Lipid, fatty acid and steroid metabolism; Electron transport
Cyp2a5	−5.86	−3.67	Lipid, fatty acid and steroid metabolism; Lipid, fatty acid and steroid metabolism; Electron transport
Mylpf	−5.59	−6.28	Muscle contraction; Developmental processes; Cell structure and motility
Myl3	−5.59	−5.29	Muscle contraction
Tpm2	−5.48	−4.39	Muscle contraction; Developmental processes; Cell structure and motility
Mb	−4.44	−2.06	Transport; Blood circulation and gas exchange
Gsn	−4.25	−1.65	Cell structure and motility
Aldh3a1	−4.10	−5.08	Other metabolism
H2-Eb1	−3.92	1.93	Immunity and defense
Tcap	−3.60	−2.24	Protein metabolism and modification; Cell structure and motility
Igfbp6	−3.45	−1.24	Signal transduction; Homeostasis
Sln	−3.39	−1.46	Biological process unclassified
Acaa1b	−3.39	−1.97	Protein metabolism and modification
Ltbp4	−3.31	−1.84	Signal transduction; Sensory perception; Developmental processes
Actc1	−3.20	−2.11	Intracellular protein traffic; Transport; Cell cycle; Cell structure and motility
Tnnc1	−3.19	−1.78	Signal transduction; Muscle contraction; Developmental processes
Pon1	−3.10	−2.43	Phosphate metabolism; Immunity and defense
Csrp3	−3.07	−1.42	Developmental processes
Rptn	−3.06	−3.40	Biological process unclassified
Epas1	−3.05	−1.89	Nucleoside, nucleotide and nucleic acid metabolism; Developmental processes
Atp2a1	−3.04	−3.33	Transport; Homeostasis
Ckm	−3.03	−2.32	Muscle contraction

coniosis and lung cancer due to their long stay in the lung.[18–21] For this reason, engineers are continuously trying to develop SiNPs which have optimal clearance with low toxicity.[1,2]

The surface charge may be one of factors causing cellular toxicity. Some researchers have reported that SiNPs that carry a positive charge are more likely to function as DNA carriers for gene transfection.[22,23] In the present study, the potential zeta value of SiNPs was −12.76 mV, and they entered into alveolar macrophages through nonspecific phagocytosis. We assume that SiNPs of positive charge may have different affinity for cell membranes to that of negatively charged SiNPs, so the toxicity between differently charged nanoparticles would also be different.

The outbreak of environment-related disease is caused by destruction of immune balance by the xenobiotics inflowing into the body. In this study, we would like to identify whether SiNPs induce Th1 response or Th2 response. Cell distribution in lymphocytes is changed during the immune response to protect the body from an inflow of xenobiotics.[24–26] For example, a single instillation of a multi-walled carbon nanotube (MWCNT) caused an increase in the proportion of B cells in both blood and spleen.[13] The proportion of B cells in blood lymphocytes was 45.97% in the control group and 80.84% in the MWCNT-treated group. In the spleen, B cells comprised 56.97% of the lympho-

cytes in the control and 68.93% in the MWCNT-treated group. After a single intratracheal instillation of titanium nanoparticles, B cell proliferation was also observed, and the ratio of $CD4^+$ T cells to $CD8^+$ T cells was decreased, which overall meant an increase in CD8+.[27] Up-regulation of antibody formation by N-Acetyl-D-glucosamine-coated polyamidoamine dendrimers is triggered by NK cell stimulation,[28] nanoparticle formulated alpha-galactosylceramide activates NKT cells without inducing allergy,[29] and G3139 lipid nanoparticles promoted proliferation of NK cells.[30] In our previous study, we observed that SiNPs increased the secretion of pro-inflammatory cytokines and the distribution of NK cells inducing serious cytotoxicity in peritoneal macrophage cells.[31] In the present study, SiNPs increased the distribution of NK and NKT cells to about 178.3 and 318.3%, respectively, compared to the control. The distribution of cytotoxic T cells was markedly increased. NK and NKT cells are a type of cytotoxic lymphocyte that constitutes a major component of the innate immune system, and up to 80% of NK cells express CD8+.

The secretion of cytokines is closely associated with the outbreak of adverse health effects caused by exposure to xenobiotics.[14,31–33] In previous our study, SiNPs intraperitoneally injected increased the secretion of IL-1β and TNF-α by 25.1 and 17.6 fold, respectively, in blood 24 hr after injection.[31] However, ultrafine amorphous silica at a 2 mg/kg dose did not induce gene expression of IL-4, IL-10, IL-13 or IFN-γ in lungs of day 1 after instillation.[14] In the present study, the secretion of pro-inflammatory, Th0 type, and Th1 type cytokines in BAL fluid were increased very markedly on day 1. In particular, the level of IL-6 increased by 854.5 fold relative to the control group. IL-6 is mainly secreted by macrophages, T cells, and endothelial cells, and it plays an important role in the acute phase response. On day 7, gene expression of SAA3 was up-regulated to levels 60 times higher than the control level. The expression level then decreased to normal by day 28. SAA proteins are involved in acute-phase responses and are synthesized in the liver during inflammatory reactions, in response to IL-6. It was also expressed primarily in the airway epithelium, bronchial glands, perichondrium of bronchial cartilage, and vascular smooth muscle cells of the lung. According to prior reports, SAA3 mRNA increased 13–15 fold in the ventilated lung when challenged with ovalbumin.[34] In the present study, the body weight of mice treated with SiNPs was apparently decreased compared with that of the control group on day 1 after instillation. In this point, we also guess that the decreases in weight gain may have resulted from the severe acute inflammatory response induced by instillation of SiNPs.

Previous research has shown TGF-β to be involved in wound repair processes and in initiating inflammatory reactions as well as in their resolution.[35] The over-expression of TGF-β leads to progressive pulmonary fibrosis accompanied by a marked up-regulation of protease inhibitors such as TIMP.[36] MMPs are a major group of proteases known to regulate the extracellular matrix, and their importance has been suggested in the process of lung disease associated with tissue remodeling.[37–42] In previous study, Choi *et al.* reported that the instillation of SiNPs induced early fibrotic lesions, with the expression of TIMP and MMPs in lung of mouse.[14] It is known that lung fibrosis is a kind of autoimmune disease, and the immune system mistakes some part of the body as a pathogen and attacks it, in some cases of, produce antibody against it. In the present study, SiNPs markedly increased the secretion of TGF-β, and significantly induced the gene expression of MMPs and TIMP on day 1, which may be an indicator of tissue damage. The increase of B cell and IgE also was marked on day 7, which may be an indicator of antibody production.

Furthermore, that of genes down-regulated on day 7 remained similar level until day 28 while the expression of up-regulated genes was recovered to control level on day 28. Based on these results, we guess that subchronic toxic response depends on down-regulated genes while initial toxic response by SiNPs depends on up-regulated genes.

In conclusion, we suggest that a single instillation of SiNPs shows a subchronic inflammatory response and tissue damage including cytokine elevation, histopathological changes, the stimulation of NK cells, and the induction of many genes related with inflammatory responses.

REFERENCES

1) Arts, J. H., Muijser, H., Duistermaat, E., Junker, K. and Kuper, C. F. (2007) Five-day inhalation toxicity study of three types of synthetic amorphous silicas in Wistar rats and post-exposure evaluations for up to 3 months. *Food Chem. Toxicol.*, **45**, 1856–1867.
2) Fubini, B. and Hubbard, A. (2003) Reactive oxygen

species (ROS) and reactive nitrogen species (RNS) generation by silica in inflammation and fibrosis. *Free Radic. Biol. Med.*, **34**, 1507–1516.
3) McLaughlin, J. K., Chow, W. H. and Levy, L. S. (1997) Amorphous silica: a review of health effects from inhalation exposure with particular reference to cancer. *J. Toxicol. Environ. Health*, **50**, 553–566.
4) Barik, T. K., Sahu, B. and Swain, V. (2008) Nanosilica-from medicine to pest control. *Parasitol. Res.*, **103**, 253–258.
5) Rahman, A., Seth, D., Mukhopadhyaya, S. K., Brahmachary, R. L., Ulrichs, C. and Goswami, A. (2009) Surface functionalized amorphous nanosilica and microsilica with nanopores as promising tools in biomedicine. *Naturwissenschaften*, **96**, 31–38.
6) Van Hoecke, K., De Schamphelaere, K. A., Van der Meeren, P., Lucas, S. and Janssen, C. R. (2008) Ecotoxicity of silica nanoparticles to the green alga Pseudokirchneriella subcapitata: importance of surface area. *Environ. Toxicol. Chem.*, **27**, 1948–1957.
7) Chang, J. S., Chang, K. L., Hwang, D. F. and Kong, Z. L. (2007) In vitro cytotoxicity of silica nanoparticles at high concentrations strongly depends on the metabolic activity type of the cell line. *Environ. Sci. Technol.*, **41**, 2064–2068.
8) Eom, H. J. and Choi, J. (2009) Oxidative stress of silica nanoparticles in human bronchial epithelial cell, Beas-2B. *Toxicol. In Vitro*, **23**, 1326–1332.
9) Jin, Y., Kannan, S., Wu, M. and Zhao, J. X. (2007) Toxicity of luminescent silica nanoparticles to living cells. *Chem. Res. Toxicol.*, **20**, 1126–1133.
10) Lin, W., Huang, Y., Zhou, X. D. and Ma, Y. (2006) In vitro toxicity of silica nanoparticles in human lung cancer cells. *Toxicol. Appl. Pharmacol.*, **217**, 252–259.
11) DiMatteo, M., Antonini, J. M., Van Dyke, K. and Reasor, M. J. (1996) Characteristics of the acute-phase pulmonary response to silica in rats. *J. Toxicol. Environ. Health*, **47**, 93–108.
12) Kaewamatawong, T., Shimada, A., Okajima, M., Inoue, H., Morita, T., Inoue, K. and Takano, H. (2006) Acute and subacute pulmonary toxicity of low dose of ultrafine colloidal silica particles in mice after intratracheal instillation. *Toxicol. Pathol.*, **34**, 958–965.
13) Park, E. J., Cho, W. S., Jeong, J., Yi, J., Choi, K. and Park, K. (2009) Pro-inflammatory and potential allergic responses resulting from B cell activation in mice treated with multi-walled carbon nanotubes by intratracheal instillation. *Toxicology*, **259**, 113–121.
14) Choi, M., Cho, W. S., Han, B. S., Cho, M., Kim, S. Y., Yi, J. Y., Ahn, B., Kim, S. H. and Jeong, J. (2008) Transient pulmonary fibrogenic effect induced by intratracheal instillation of ultrafine amorphous silica in A/J mice. *Toxicol. Lett.*, **182**, 97–101.
15) Hauck, T. S., Ghazani, A. A. and Chan, W. C. (2008) Assessing the effect of surface chemistry on gold nanorod uptake, toxicity, and gene expression in mammalian cells. *Small*, **4**, 153–159.
16) Park, E. J., Kim, H., Kim, Y., Yi, J., Choi, K. and Park, K. (2010) Inflammatory responses may be induced by a single intratracheal instillation of iron nanoparticlesd in mice. *Toxicology*, **275**, 65–71.
17) Vendrame, M., Gemma, C., Pennypacker, K. R., Bickford, P. C., Davis, S. C., Sanberg, P. R. and Willing, A. E. (2006) Cord blood rescues stroke-induced changes in splenocyte phenotype and function. *Exp. Neurol.*, **199**, 191–200.
18) Brown, T. (2009) Silica exposure, smoking, silicosis and lung cancer-complex interactions. *Occup. Med. (Lond.)*, **59**, 89–95.
19) Hamiton, R. F., Jr., Thakur, S. A. and Holian, A. (2008) Silica binding and toxicity in alveolar macrophages. *Free Radic. Biol. Med.*, **44**, 1246–1258.
20) Merget, R., Bauer, T., Küpper, H. U., Philippou, S., Bauer, H. D., Breitstadt, R. and Bruening, T. (2002) Health hazards due to the inhalation of amorphous silica. *Arch. Toxicol.*, **75**, 625–634.
21) Castranova, V., Porter, D., Millecchia, L., Ma, J. Y., Hubbs, A. F. and Teass, A. (2002) Effect of inhaled crystalline silica in a rat model: time course of pulmonary reactions. *Mol. Cell. Biochem.*, **234-235**, 177–184.
22) Kneuer, C., Sameti, M., Bakowsky, U., Schiestel, T., Schirra, H., Schmidt, H. and Lehr, C. M. (2000) A nonviral DNA delivery system based on surface modified silica-nanoparticles can efficiently transfect cells in vitro. *Bioconjug. Chem.*, **11**, 926–932.
23) Ravi Kumar, M. N., Sameti, M., Mohapatra, S. S., Kong, X., Lockey, R. F., Bakowsky, U., Lindenblatt, G., Schmidt, H. and Lehr, C. M. (2004) Cationic silica nanoparticles as gene carriers: synthesis, characterization and transfection efficiency in vitro and in vivo. *J. Nanosci. Nanotechnol.*, **4**, 876–881.
24) Kozłowska, E., Krzystyniak, K., Drela, N., Grabarczyk, P. and Izdebska-Szymona, K. (1996) Thymus-directed immunotoxicity of airborne dust particles from upper Silesia (Poland) under acute extrapulmonary studies in mice. *J. Toxicol. Environ. Health*, **49**, 563–579.
25) Richters, A. and Damji, K. S. (1988) Changes in T-lymphocyte subpopulations and natural killer cells following exposure to ambient levels of nitrogen dioxide. *J. Toxicol. Environ. Health*, **25**, 247–256.
26) Smialowicz, R. J., Luebke, R. W., Riddle, M. M.,

Rogers, R. R. and Rowe, D. G. (1985) Evaluation of the immunotoxic potential of chlordecone with comparison to cyclophosphamide. *J. Toxicol. Environ. Health*, **15**, 561–574.
27) Park, E. J., Yoon, J., Choi, K., Yi, J. and Park, K. (2009) Induction of chronic inflammation in mice treated with titanium dioxide nanoparticles by intratracheal instillation. *Toxicology*, **260**, 37–46.
28) Hulikova, K., Benson, V., Svoboda, J., Sima, P. and Fiserova, A. (2009) N-Acetyl-D-glucosamine-coated polyamidoamine dendrimer modulates antibody formation via natural killer cell activation. *Int. Immunopharmacol.*, **9**, 792–799.
29) Thapa, P., Zhang, G., Xia, C., Gelbard, A., Overwijk, W. W., Liu, C., Hwu, P., Chang, D. Z., Courtney, A., Sastry, J. K., Wang, P. G., Li, C. and Zhou, D. (2009) Nanoparticle formulated alpha-galactosylceramide activates NKT cells without inducing anergy. *Vaccine*, **27**, 3484–3488.
30) Pan, X., Chen, L., Liu, S., Yang, X., Gao, J. X. and Lee, R. J. (2009) Antitumor activity of G3139 lipid nanoparticles (LNPs). *Mol. Pharm.*, **6**, 211–220.
31) Park, E. J. and Park, K. (2009) Oxidative stress and pro-inflammatory responses induced by silica nanoparticles in vivo and in vitro. *Toxicol. Lett.*, **184**, 18–25.
32) Mayeux, P. R. (1997) Pathobiology of lipopolysaccharide. *J. Toxicol. Environ. Health*, **51**, 415–435.
33) Reinhart, P. G. and Gairola, C. G. (1997) Amiodarone-induced pulmonary toxicity in Fischer rats: release of tumor necrosis factor alpha and transforming growth factor beta by pulmonary alveolar macrophage. *J. Toxicol. Environ. Health*, **52**, 353–365.
34) Wilson, T. C., Bachurski, C. J., Ikegami, M., Jobe, A. H. and Kallapur, S. G. (2005) Pulmonary and systemic induction of SAA3 after ventilation and endotoxin in preterm lambs. *Pediatr. Res.*, **58**, 1204–1209.
35) Lawrence, D. A. (1996) Transforming growth factor-beta: a general review. *Eur. Cytokine Netw.*, **7**, 363–374.
36) Gauldie, J., Kolb, M., Ask, K., Martin, G., Bonniaud, P. and Warburton, D. (2006) Smad3 signaling involved in pulmonary fibrosis and emphysema. *Proc. Am. Thorac. Soc.*, **3**, 696–702.
37) Cawston, T., Carrere, S., Catterall, J., Duggleby, R., Elliott, S., Shingleton, B. and Rowan, A. (2001) Matrix metalloproteinases and TIMPs: properties and implications for the treatment of chronic obstructive pulmonary disease. *Novartis Foundation Symposium*, **234**, 205–218.
38) Clark, I. M., Swingler, T. E., Sampieri, C. L. and Edwards, D. R. (2008) The regulation of matrix metalloproteinases and their inhibitors. *Int. J. Biochem. Cell. Biol.*, **40**, 1362–1378.
39) Demedts, I. K., Brusselle, G. G., Bracke, K. R., Vermaelen, K. Y. and Pauwels, R. A. (2005) Matrix metalloproteinases in asthma and COPD. *Curr. Opin. Pharmacol.*, **5**, 257–263.
40) Gueders, M. M., Foidart, J. M., Noel, A. and Cataldo, D. D. (2006) Matrix metalloproeinases (MMPs) and tissue inhibitors of MMPs in the respiratory tract: potential implications in asthma and other lung diseases. *Eur. J. Pharmacol.*, **533**, 133–144.
41) Lagente, V., Manoury, B., Nénan, S., Le Quémen, C., Martin-Chouly, C. and Boichot, E. (2005) Role of marix metalloproteinases in the development of airway inflammation and remodeling. *Braz. J. Med. Biol. Res.*, **38**, 1521–1530.
42) Ohbayashi, H. (2002) Matrix metalloproteinases in lung diseases. *Curr. Protein Pept. Sci.*, **3**, 409–421.